

A lattice calculation of the branching ratio for some of the exclusive modes of $b \rightarrow s\gamma$.

UKQCD Collaboration*

K.C. Bowler, N.M. Hazel, D.S. Henty, H. Hoerber, R.D. Kenway, D.G. Richards,
H.P. Shanahan, J.N. Simone

Department of Physics, The University of Edinburgh, Edinburgh EH9 3JZ, Scotland

J.M. Flynn, B.J. Gough

Department of Physics, University of Southampton, Southampton SO17 1BJ, UK

(hep-lat/9407013, February 1995)

Abstract

We calculate the leading-order matrix element for exclusive decays of $b \rightarrow s\gamma$ in the quenched approximation of lattice QCD on a $24^3 \times 48$ lattice at $\beta=6.2$, using an $O(a)$ -improved fermion action. The matrix element is used to extract the on-shell form factor $T_1(q^2=0)$ for $B \rightarrow K^*\gamma$ and $B_s \rightarrow \phi\gamma$, using two different assumptions about the q^2 dependence of the form factors for these decays. For $B \rightarrow K^*\gamma$, $T_1(q^2=0)$ is determined to be $0.159_{-33}^{+34} \pm 0.067$ or $0.124_{-18}^{+20} \pm 0.022$ in the two cases. We find the results to be consistent (in the Standard Model) with the CLEO experimental branching ratio of $BR(B \rightarrow K^*\gamma) = (4.5 \pm 1.5 \pm 0.9) \times 10^{-5}$.

Typeset using REVTeX

*kcb@th.ph.ed.ac.uk, jflynn@southampton.ac.uk

I. INTRODUCTION

A. The Standard Model and New Physics

Theoretical interest in the rare decay $B \rightarrow K^*\gamma$ as a test of the Standard Model has been renewed by the experimental results of the CLEO collaboration [1]. For the first time, this mode has been positively identified and a preliminary determination of its branching ratio given.

The radiative decays of the B meson are remarkable for several reasons. The decay $B \rightarrow K^*\gamma$ arises from the flavour-changing quark-level process $b \rightarrow s\gamma$, which occurs through penguin diagrams at one-loop in the Standard Model. As a result, the decay is a purely quantum effect and a subtle test of the Standard Model. The process is also sensitive to new physics appearing through virtual particles in the internal loops. Existing bounds on the $b \rightarrow s\gamma$ branching ratio have been used to place constraints on supersymmetry (SUSY) [2–8] and other extensions of the Standard Model (SM) [9,10]. A comprehensive review of these results can be found in [11]. Finally, it is also remarkable that this rare process has a sufficiently large branching ratio to be detected experimentally. Thus, *accurate* experimental measurements and *accurate* theoretical calculations of these decays could soon probe new physics at comparatively low energies.

In order to compare the experimental branching ratio with a theoretical prediction it is necessary to know the relevant hadronic matrix elements. These have been estimated using a wide range of methods, including relativistic and nonrelativistic quark models [12–14], two-point and three-point QCD sum rules [15–20] and heavy quark symmetry [21], but there remains some disagreement between the different results. It is therefore of interest to perform a direct calculation of the matrix elements using lattice QCD. The viability of the lattice approach was first demonstrated by the work of Bernard, Hsieh and Soni [22] in 1991.

Excluding QCD contributions, the free quark decay $b \rightarrow s\gamma$ in the SM proceeds by diagrams similar to that shown in Fig.(1). The charm and top quark dominate, because the

up quark contribution to the loop is suppressed by the small CKM factor $|V_{ub}V_{us}^*|$.

If the value of the top mass is assumed, the Standard Model can be tested by deriving an independent result for $BR(B \rightarrow K^*\gamma)$. Deviations from the expected branching ratio would be an indication of contributions to the decay from physics beyond the SM, to which this decay is potentially sensitive.

Research on such contributions can be classified into supersymmetric and non-supersymmetric extensions of the SM. In the latter case, Cho and Misiak [23] considered $SU(2)_L \otimes SU(2)_R$ left-right symmetric models and found considerable variations from the SM result for a wide range of the free parameters, while Randall and Sundrum [24] found significant potential deviations from the SM in technicolour models. Anomalous $WW\gamma$ couplings in $b \rightarrow s\gamma$ have been analysed and the results found to be consistent with the SM. The bounds obtained from this approach can improve on those from direct searches [25–28]. The contributions from two Higgs doublet models [29,30] have been analysed to obtain bounds on the charged Higgs mass and $\tan\beta$, the ratio of the vacuum expectation values of the doublets [31,32].

SUSY models also involve additional Higgs doublets, but the contribution of other boson-fermion loops, in particular charginos (χ^-) with up type squarks, and gluinos (\tilde{g}) or neutralinos (χ^0) with down type squarks must also be included [2–8,33]. A thorough study of the decay in the Minimal Supersymmetric Standard model can be found in reference [8]. There are a strong contributions from chargino and gluino loops, especially for large $\tan\beta$, which interfere destructively with the Higgs contribution and allow SUSY to mimic the SM in some regions of parameter space. As a result, the current limits on $\tan\beta$ and Higgs masses are weak, but will tighten as more stringent bounds on superpartner masses are obtained.

For the rest of this paper, we shall use the SM as the appropriate model, and look for possible deviations from the experimental branching ratio. It should be noted that the lattice calculation is needed only to determine the effects of low energy QCD, and these are independent of new physics. The low energy effect of many extensions of the SM will be completely contained within the renormalisation group operator coefficients, and hence it is

straightforward to allow for contributions from different models.

B. Exclusive vs. Inclusive decay modes

The inclusive decay $B \rightarrow X_s \gamma$ is predominantly a short distance process and can be treated perturbatively in the spectator approximation. It is also possible to use Heavy Quark Effective Theory (HQET) to compute the leading $1/m_b^2$ corrections [34]. The experimental inclusive branching ratio has been determined at CLEO [35],

$$BR(B \rightarrow X_s \gamma) = (2.32 \pm 0.51 \pm 0.29 \pm 0.32) \times 10^{-4}. \quad (1)$$

The procedure for obtaining this result has a mild model dependence (the final result is a function of m_b).

In addition, the branching ratios of the exclusive decay modes of $b \rightarrow s \gamma$ can also be experimentally determined, and the present published branching ratio for $B \rightarrow K^* \gamma$ from the CLEO collaboration [1] is,

$$BR(B \rightarrow K^* \gamma) = (4.5 \pm 1.5 \pm 0.9) \times 10^{-5}. \quad (2)$$

The advantage of this measurement is that the experimental number is model independent. Theoretical calculation of the relevant exclusive matrix element requires the determination of long distance QCD contributions which cannot be determined perturbatively, but can be computed using lattice QCD.

C. The Effective Hamiltonian and Hadronic Matrix Elements

In order to determine the low energy QCD contributions to this decay, the high energy degrees of freedom must be integrated out, generating an effective $\Delta B = -1$, $\Delta S = 1$ hamiltonian. Grinstein, Springer and Wise [36] determined the hamiltonian \mathcal{H}_{eff} , to leading order in weak matrix elements,

$$\mathcal{H}_{eff} = -\frac{4G_F}{\sqrt{2}}V_{tb}V_{ts}^* \sum_{i=1}^8 C_i(\mu)O_i, \quad (3)$$

where the eight operators O_i are multiplied by the renormalisation group coefficients, $C_i(\mu)$. Six of the operators are four-quark operators and two are magnetic moment operators, coupling to the gluon and photon [37]. The operator which mediates the $b \rightarrow s\gamma$ transition is,

$$O_7 = \frac{e}{16\pi^2}m_b\bar{s}\sigma_{\mu\nu}\frac{1}{2}(1+\gamma_5)b F^{\mu\nu}. \quad (4)$$

The coefficients $C_i(\mu)$ are set by matching to the full theory at the scale $\mu = M_W$. The coefficient $C_7(m_b)$ is determined using the renormalization group to run down to the appropriate physical scale $\mu = m_b$ [38], and is approximately given by,

$$C_7(m_b) = \eta^{-16/23} \left(C_7(M_W) + \frac{58}{135}(\eta^{10/23} - 1) + \frac{29}{189}(\eta^{28/23} - 1) \right), \quad \eta = \frac{\alpha_s(m_b)}{\alpha_s(M_W)}, \quad (5)$$

where, in the Standard Model [39],

$$C_7^{SM}(M_W) = \frac{1}{2} \frac{x}{(x-1)^3} \left(\frac{2}{3}x^2 + \frac{5}{12}x - \frac{7}{12} - \frac{x}{2} \frac{(3x-2)}{(x-1)} \log x \right), \quad x = \frac{m_t^2}{M_W^2}. \quad (6)$$

The effects of scale uncertainty in the leading order approximation have been considered by Buras *et al.* [31].

To leading order, the on-shell matrix for $B \rightarrow K^*\gamma$ is given by,

$$\mathcal{M} = \frac{eG_F m_b}{2\sqrt{2}\pi^2} C_7(m_b) V_{tb} V_{ts}^* \eta^{\mu*} \langle K^* | J_\mu | B \rangle, \quad (7)$$

where,

$$J_\mu = \bar{s}\sigma_{\mu\nu}q^\nu b_R, \quad (8)$$

and η and q are the polarization and momentum of the emitted photon. As outlined by Bernard, Hsieh and Soni [22], the matrix element $\langle K^* | \bar{s}\sigma_{\mu\nu}q^\nu b_R | B \rangle$ can be parametrised by three form factors,

$$\langle K^* | J_\mu | B \rangle = \sum_{i=1}^3 C_\mu^i T_i(q^2), \quad (9)$$

where,

$$C_\mu^1 = 2\varepsilon_{\mu\nu\lambda\rho}\epsilon^\nu p^\lambda k^\rho, \quad (10)$$

$$C_\mu^2 = \epsilon_\mu(m_B^2 - m_{K^*}^2) - \epsilon \cdot q(p+k)_\mu, \quad (11)$$

$$C_\mu^3 = \epsilon \cdot q \left(q_\mu - \frac{q^2}{m_B^2 - m_{K^*}^2} (p+k)_\mu \right). \quad (12)$$

As the photon emitted is on-shell, the form factors need to be evaluated at $q^2=0$. In this limit,

$$T_2(q^2=0) = -iT_1(q^2=0), \quad (13)$$

and the coefficient of $T_3(q^2=0)$ is zero. Hence, the branching ratio can be expressed in terms of a single form factor, for example,

$$BR(B \rightarrow K^* \gamma) = \frac{\alpha}{8\pi^4} m_b^2 G_F^2 m_B^3 \tau_B \left(1 - \frac{m_{K^*}^2}{m_B^2} \right)^3 |V_{tb} V_{ts}^*|^2 |C_7(m_b)|^2 |T_1(q^2=0)|^2. \quad (14)$$

This paper concerns the evaluation of $T_1(0)$. We shall outline how matrix elements of the form $\langle V | J_\mu | P \rangle$, where $|P\rangle$ is a heavy-light pseudoscalar meson and $|V\rangle$ is a strange-light vector meson, can be calculated in lattice QCD and explain the computational details involved. We shall evaluate the form factors $T_1(q^2=0)$ and $T_2(q^2=0)$, make some statements about the systematic error, and compare the calculated value of $BR(B \rightarrow K^* \gamma)$ with the results from CLEO.

D. Heavy Quark Symmetry

We cannot directly simulate b -quarks on the lattice, as will be explained below. Instead, we calculate with a selection of quark masses near the charm mass. This means that any results for the form factors must be extrapolated to the b -quark scale. Heavy quark symmetry [40] tells us that,

$$\begin{aligned} T_1(q_{max}^2) &\sim m_P^{1/2} \\ T_2(q_{max}^2) &\sim m_P^{-1/2} \end{aligned} \quad (15)$$

as the heavy quark mass, and hence the pseudoscalar meson mass, m_P , grows infinitely large. Combining this with the relation $T_2(q^2=0) = -iT_1(q^2=0)$ constrains the q^2 dependence of the form factors.

Pole dominance ideas suggest that,

$$T_i(q^2) = \frac{T_i(0)}{(1 - q^2/m_i^2)^{n_i}} \quad (16)$$

for $i = 1, 2$, where m_i is a mass that is equal to m_P plus $1/m_P$ corrections and n_i is a power. Since $1 - q_{max}^2/m_i^2 \sim 1/m_P$ for large m_P , the combination of heavy quark symmetry and the form factor relation at $q^2 = 0$ implies that $n_1 = n_2 + 1$. Thus we could fit $T_2(q^2)$ to a constant and $T_1(q^2)$ to a single pole form or fit $T_2(q^2)$ to a single pole and $T_1(q^2)$ to a double pole. These two cases correspond to,

$$T_1(0) \sim \begin{cases} m_P^{-1/2} & \text{single pole} \\ m_P^{-3/2} & \text{double pole} \end{cases} . \quad (17)$$

As we will see, our data for $T_2(q^2)$ appear roughly constant in q^2 when m_P is around the charm scale, but have increasing dependence on q^2 as the heavy quark mass increases. We will fit to both constant and single pole behaviours for $T_2(q^2)$ below.

II. LATTICE FIELD THEORY

The hadronic matrix element $\langle V|J_\mu|P\rangle$ for the $b \rightarrow s\gamma$ transition can be obtained from the correlator $\langle 0|J_\rho^V(x)T_{\mu\nu}(y)J_P^\dagger(0)|0\rangle$, where J_P and J_ρ^V are interpolating fields for the P and V mesons, consisting of a heavy quark, h , a light quark, l , and a strange quark, s ;

$$J_P(x) = \bar{l}(x)\gamma_5 h(x), \quad (18)$$

$$J_\rho^V(x) = \bar{l}(x)\gamma_\rho s(x), \quad (19)$$

$$T_{\mu\nu}(y) = \bar{s}(y)\sigma_{\mu\nu} h(y). \quad (20)$$

The full matrix element $\langle V|\bar{s}\sigma_{\mu\nu}\frac{1}{2}(1 + \gamma_5)h|P\rangle$ can be derived using the Minkowski space relation,

$$\gamma^5 \sigma^{\mu\nu} = \frac{i}{2} \varepsilon^{\mu\nu\rho\lambda} \sigma_{\rho\lambda}. \quad (21)$$

In Euclidean space, the correlator $\langle 0 | J_\rho^V(x) T_{\mu\nu}(y) J_P^\dagger(0) | 0 \rangle$ can be computed numerically using the functional integral,

$$\langle 0 | J_\rho^V(x) T_{\mu\nu}(y) J_P^\dagger(0) | 0 \rangle = \frac{1}{Z} \int \mathcal{D}A \mathcal{D}q \mathcal{D}\bar{q} J_\rho^V(x) T_{\mu\nu}(y) J_P^\dagger(0) \exp(-S[A, q, \bar{q}]), \quad (22)$$

$$= \frac{1}{Z} \int \mathcal{D}A \text{Tr} (\gamma_5 H(0, y) \sigma_{\mu\nu} S(y, x) \gamma_\rho L(x, 0)) \exp(-S_{\text{eff}}), \quad (23)$$

where $S[A, q, \bar{q}]$ is the QCD action and $S(y, x)$, $H(y, x)$, $L(y, x)$ are the propagators from x to y for the s , h and l quarks. Working in momentum space, we calculate the three-point correlator,

$$C_{\rho\mu\nu}^{3pt}(t, t_f, \vec{p}, \vec{q}) = \sum_{\vec{x}, \vec{y}} e^{i\vec{p}\cdot\vec{x}} e^{-i\vec{q}\cdot\vec{y}} \langle J_P(t_f, \vec{x}) T_{\mu\nu}(t, \vec{y}) J_{V\rho}^\dagger(0) \rangle \quad (24)$$

$$\xrightarrow{t, t_f-t, T \rightarrow \infty} \sum_{\epsilon} \frac{Z_P}{2E_P} \frac{Z_V}{2E_V} e^{-E_P(t_f-t)} e^{-E_V t} \epsilon_\rho \langle P(p) | \bar{h} \sigma_{\mu\nu} s | V(k, \epsilon) \rangle. \quad (25)$$

To obtain the matrix element $\langle P(p) | \bar{h} \sigma_{\mu\nu} s | V(k) \rangle$, we take the ratio,

$$C_{\rho\mu\nu}(t, t_f, \vec{p}, \vec{q}) = \frac{C_{\rho\mu\nu}^{3pt}(t, t_f, \vec{p}, \vec{q})}{C_P^{2pt}(t_f - t, \vec{p}) C_V^{2pt}(t, \vec{p} - \vec{q})}, \quad (26)$$

where the two-point correlators are defined as,

$$\begin{aligned} C_P^{2pt}(t, \vec{p}) &= \sum_{\vec{x}} e^{i\vec{p}\cdot\vec{x}} \langle J_P^\dagger(t, \vec{x}) J_P(0) \rangle \\ &= \frac{Z_P^2}{2E_P} (e^{-E_P t} + e^{-E_P(T-t)}), \end{aligned} \quad (27)$$

$$\begin{aligned} C_V^{2pt}(t, \vec{k}) &= -\left(\frac{1}{3}\right) \sum_{\vec{x}} e^{i\vec{k}\cdot\vec{x}} \langle J_{V\sigma}^\dagger(t, \vec{x}) J_V^\sigma(0) \rangle \\ &= \frac{Z_V^2}{2E_V} (e^{-E_V t} + e^{-E_V(T-t)}). \end{aligned} \quad (28)$$

By time reversal invariance and assuming the three points in the correlators of Eq.(26) are sufficiently separated in time, a term proportional to the required matrix element dominates:

$$C_{\rho\mu\nu} \xrightarrow{t, t_f-t, T \rightarrow \infty} \frac{1}{Z_P Z_V} \sum_{\epsilon} \epsilon_\rho \langle V(k, \epsilon) | \bar{s} \sigma_{\mu\nu} h | P(p) \rangle + \dots, \quad (29)$$

and $C_{\rho\mu\nu}$ approaches a plateau. The three-point correlator is calculated in its time reversed form to allow the use of previously calculated light propagators. The factors Z_P , Z_V and the energies of the pseudoscalar and vector particles are obtained from fits to the two-point Euclidean correlators.

In order to simulate this decay on a sufficiently finely spaced lattice, vacuum polarisation effects were discarded and the gauge field configurations generated in the quenched approximation. The decays $D \rightarrow Ke\nu$, $D \rightarrow K^*e\nu$, and $D_s \rightarrow \phi e\nu$ have been calculated in the quenched approximation [41–43] and have been found to be in relatively good agreement with experiment. It is therefore quite plausible to assume that the systematic error from the quenched approximation for this calculation would be of a similar size.

The matrix element $\langle K^* | \bar{s} \sigma_{\mu\nu} q^\nu b_R | B \rangle$ cannot be directly calculated as realistic light quarks cannot be simulated owing to critical slowing down in determining the propagator for small masses. Instead light quarks are simulated at a number of masses approximately that of the strange quark mass, and any result is extrapolated to the chiral limit. Furthermore, b quarks cannot be simulated directly as the b -quark mass is greater than the inverse lattice spacing (2.73(5) GeV), and the variation of the propagator would occur over lengths smaller than the lattice spacing. As a result, heavy quarks are simulated with masses around the charm quark mass, and the results extrapolated to m_b . Hence, $\langle V | J_\mu | P \rangle$ has to be calculated at a number of different light, strange and heavy quark masses.

III. COMPUTATIONAL DETAILS

Sixty $SU(3)$ gauge configurations were generated in the quenched approximation for a $24^3 \times 48$ lattice at $\beta = 6.2$. These configurations were generated with periodic boundary conditions using the hybrid over-relaxed algorithm, and the standard discretised gluon action, defined in [44]. The configurations were separated by 400 compound sweeps, starting at sweep number 2800. The inverse lattice spacing was determined to be 2.73(5) GeV, by evaluating the string tension [45]. In physical units, this corresponds to a spacing of ap-

proximately 0.07 fm and a spatial size of 1.68 fm. In order to simulate heavy quarks whose masses are approaching the inverse lattice spacing, the $O(a)$ -improved fermion action of Sheikholeslami and Wohlert [46] (also referred to as the clover action) was used. This is defined as,

$$S_F^C = S_F^W - i\frac{\kappa}{2} \sum_{x,\mu,\nu} \bar{q}(x) F_{\mu\nu}(x) \sigma_{\mu\nu} q(x), \quad (30)$$

where S_F^W is the standard Wilson fermion action [45,47] and $F_{\mu\nu}$ is a lattice definition of the field strength tensor, which we take to be the sum of the four untraced plaquettes in the $\mu\nu$ plane open at the point x ,

$$F_{\mu\nu}(x) = \frac{1}{4} \sum_{\square=1}^4 \frac{1}{2i} \left[U_{\square\mu\nu}(x) - U_{\square\mu\nu}^\dagger(x) \right]. \quad (31)$$

In using this action, all observables with fermion fields q, \bar{q} must be “rotated”,

$$\begin{aligned} q(x) &\rightarrow \left(1 - \frac{1}{2} \overrightarrow{\Delta} \right) q(x), \\ \bar{q}(x) &\rightarrow \bar{q}(x) \left(1 + \frac{1}{2} \overleftarrow{\Delta} \right), \end{aligned} \quad (32)$$

where Δ_μ is the discretised covariant derivative, operating on the quark fields as,

$$\begin{aligned} \overrightarrow{\Delta}_\mu q(x) &= \frac{1}{2} \left(U_\mu(x) q(x + \mu) - U_\mu^\dagger(x - \mu) q(x - \mu) \right), \\ \bar{q}(x) \overleftarrow{\Delta}_\mu &= \frac{1}{2} \left(\bar{q}(x + \mu) U_\mu^\dagger(x) - \bar{q}(x - \mu) U_\mu(x - \mu) \right). \end{aligned} \quad (33)$$

This action eliminates the tree level $O(ma)$ -error of the Wilson action [48], which can be significant for heavy quark systems [49,50].

For each configuration, quark propagators were calculated using the over-relaxed minimal residual algorithm with red-black preconditioning for $\kappa = 0.14144$, 0.14226 and 0.14262, using periodic boundary conditions in the spatial directions and anti-periodic boundary conditions in the temporal direction. Smearing was not used in the calculation of these light propagators. The first two κ values can be used to interpolate to the strange quark mass which corresponds to $\kappa = 0.1419(1)$ [51]. The third κ value, corresponding to a somewhat

lighter quark, was used in conjunction with the others in order to test the behaviour of the data in the chiral limit.

Heavy propagators, for $\kappa_h = 0.121, 0.125, 0.129$ and 0.133 , were evaluated using timeslice 24 of some of the above propagators as the source. For $\kappa_h = 0.121$ and 0.129 , the propagators for all of the light κ values were used. For $\kappa_h = 0.125$ and 0.133 , the propagators for $\kappa = 0.14144$ and 0.14226 were used. To reduce excited state contamination, these sources were smeared using the gauge invariant Jacobi algorithm [52], with an r.m.s. smearing radius of 5.2. Because of memory limitations, these propagators were evaluated only for timeslices 7 to 16 and 32 to 41.

Using these propagators, the three point correlators were evaluated. The spatial momentum \mathbf{p} was chosen to be $(0, 0, 0)$ or $(\pi/12, 0, 0)$ (the lowest unit of momentum in lattice units that can be injected). All possible choices of \mathbf{q} were calculated such that the magnitude of the spatial momentum of the vector meson \mathbf{k} was less than $\sqrt{2}\pi/12$. This is because the signal of light hadrons degrades rapidly as the momentum is increased [53].

In order to obtain $\langle V|\bar{s}\sigma_{\mu\nu}h|P\rangle$, the decay constant and energy were determined for the pseudoscalar of each heavy–light κ combination and the vector of each possible light κ combination, for all possible momenta used. The process of extracting these is well understood and has been discussed in detail elsewhere [51]. As the two point functions are periodic, a correlator at a time $0 \leq t \leq 24$ was averaged with the same correlator at $48 - t$ to improve the statistical sample. This “folded” data was fitted to Eq.(27) or Eq.(28) for timeslices 15 to 23. For both the two point and three point functions we utilised the discrete symmetries C , P and T (folding) wherever possible, in addition to averaging over equivalent momenta. The statistical errors for all correlators were determined by the bootstrap procedure [54], using 1000 bootstrap subsamples from the original configurations. The finite renormalization needed for the lattice–continuum matching of the $\sigma_{\mu\nu}$ operator has been calculated [55] but has a negligible effect here ($O(2\%)$) and was not included. It introduces a small correction to the branching ratio which is considered in the conclusions.

As outlined in the previous section, the weak matrix elements $C_{\rho\mu\nu}$ were extracted from

the three point data and the fits to the two point data. Having divided out the contributions from the two point amplitudes and energies, the matrix element $\langle V|\bar{s}\sigma_{\mu\nu}h|P\rangle$ was isolated. These matrix elements were combined to determine the form factors $T_1(q^2)$, $T_2(q_{max}^2)$ and $T_2(q^2)$. Each form factor was extracted by a correlated fit to a constant for timeslices 11, 12 and 13.

IV. RESULTS

The data for unphysical masses, and off-shell photons must be combined to isolate the form factors and extrapolate to the physical regime. It is clear from Eq.(13) and Eq.(14) that the branching ratio can be evaluated from $T_1(q^2=0; m_B; m_{K^*})$ or $T_2(q^2=0; m_B; m_{K^*})$. As demonstrated in a previous paper [56], the evaluation of $T_1(q^2=0; m_P; m_{K^*})$ is relatively straightforward, and $T_2(q^2=0; m_P; m_{K^*})$ can be determined in a similar way. To test heavy quark scaling, we also extracted the form factor T_2 at maximum recoil, where $q^2 = q_{max}^2 = (m_P - m_V)^2$, in the same way as Bernard *et al.* [57]. These form factors were extrapolated to the physical mass $m_P = m_B$, and an estimate of systematic errors in the extrapolation made by comparing different methods.

A. Extraction of form factors

1. $T_1(q^2)$

The form factor T_1 can be conveniently extracted from the matrix elements by considering different components of the relation,

$$4(k^\alpha p^\beta - p^\alpha k^\beta)T_1(q^2) = \varepsilon^{\alpha\beta\rho\mu}C_{\rho\mu\nu}q^\nu. \quad (34)$$

We see a plateau in T_1 about $t = 12$. The use of smeared operators for the heavy quarks provides a very clean signal, with stable plateaus forming before timeslice 11. The data for

the heaviest of our light quarks, $\kappa_l = \kappa_s = 0.14144$, with the smallest statistical errors, are shown in Fig.(2).

The form factor is evaluated for each of the five possible values of q^2 . We fit $T_1(q^2)$ to a pole or dipole model in order to obtain the on-shell form factor $T_1(q^2=0)$,

$$T_1(q^2) = \frac{T_1(q^2=0)}{1 - q^2/m^2}, \quad T_1(q^2) = \frac{T_1(q^2=0)}{(1 - q^2/m^2)^2}. \quad (35)$$

We allow for correlations between the energies of the vector and pseudoscalar particles and T_1 at each q^2 . An example of such a fit, for $\kappa_l = \kappa_s = 0.14144$, is shown in Fig.(5) and the full set of fit parameters and their $\chi^2/\text{d.o.f.}$ are shown in tables I and II.

The chiral limit behaviour of $T_1(q^2=0; m_P; m_V)$, interpolated from a single pole fit, was explored for $\kappa_h = 0.121$ and 0.129 , in our earlier work [56]. To test for approximate spectator quark independence, we compared the single pole fits of the form factor to the two functions,

$$T_1(q^2=0; m_{q,light}) = a + bm_l, \quad (36)$$

$$T_1(q^2=0; m_{q,light}) = c, \quad (37)$$

where m_l is the lattice pole mass,

$$m_l = \frac{1}{2} \left(\frac{1}{\kappa} - \frac{1}{\kappa_{crit}} \right), \quad (38)$$

and $\kappa_{crit} = 0.14315(2)$ [58]. The linear coefficient b was found to be consistent with zero for each combination of κ_s and κ_h (see Fig.6). From table V, the $\chi^2/\text{d.o.f.}$ for both fits are similar, indicating that for the data available, the assumption that the form factor is a constant, independent of the spectator quark mass, is valid. Hence, the data for $\kappa_l = 0.14144$ was used for the chiral limit, and a simple linear interpolation carried out between $\kappa_s = 0.14144$ and 0.14226 for the strange quark, in order to obtain $T_1(q^2=0; m_P; m_{K^*})$. These results are listed in the columns labelled (b) and (c) in table VIII.

2. $T_2(q^2)$

The form factor T_2 can be extracted from the matrix elements using the same procedure as T_1 , by considering the different components of,

$$(m_P^2 - m_V^2)T_2(q^2; m_P; m_V) = C_{iiv}q^\nu, \quad (39)$$

for all i (not summed) such that $q^i = 0$. A typical plateau for T_2 is shown in Fig.(3). We extract T_2 for a range of q^2 as shown in Fig.(7).

Fig.(7) shows that $T_2(q^2)$ is roughly constant as a function of q^2 for our data, with heavy quark masses around the charm mass. We fit T_2 to a constant: we can then compare with the value of $T_1(q^2 = 0)$ where T_1 is fitted with a single pole form. We also fit T_2 to a single pole form (as shown in the figure) and compare with $T_1(q^2 = 0)$ when T_1 is fitted with a double pole form. The results of the fits for T_2 are shown in tables III and IV, and the chiral extrapolations for the single pole fit in table VI. The pole mass is found to be large, and a linear behaviour holds well for all possible q^2 , including q_{max}^2 , as shown in Fig.(7). Once again the data for $k_l = 0.14144$ was used for the chiral limit and the results are listed in the columns labelled (d) and (e) in table VIII.

The ratio $T_1(q^2=0; m_P; m_{K^*})/T_2(q^2=0; m_P; m_{K^*})$ is shown in Fig.(9). The two sets of points show T_1 fitted to a double pole form and T_2 to a single pole or T_1 fitted to a single pole and T_2 constant. The ratio should be 1, in accordance with the identity $T_2(0) = -iT_1(0)$, Eq.(13). We find greater consistency from the double-pole/single-pole fit.

3. $T_2(q_{max}^2)$

The evaluation of $T_2(q_{max}^2; m_P; m_V)$ is also straightforward, since at zero momentum, $\mathbf{p}=\mathbf{0}$, $\mathbf{k}=\mathbf{0}$, the contributions from other form factors vanish,

$$\begin{aligned} (m_P + m_V)T_2(q_{max}^2) &= C_{110}(\mathbf{p} = \mathbf{0}, \mathbf{k} = \mathbf{0}), \\ &= C_{220}(\mathbf{p} = \mathbf{0}, \mathbf{k} = \mathbf{0}), \\ &= C_{330}(\mathbf{p} = \mathbf{0}, \mathbf{k} = \mathbf{0}). \end{aligned} \quad (40)$$

An example of this data is shown in Fig.(4). The behaviour of $T_2(q_{max}^2; m_P; m_V)$ as a function of the spectator quark mass was examined at $\kappa_h = 0.121$ and 0.129 in the same way as for $T_1(q^2=0)$. It was again found that the linear coefficient b was consistent with zero for each

combination of κ_s and κ_h : see Fig.(8) for an example. From table VII, the $\chi^2/\text{d.o.f.}$ for both fits are seen to be similar, indicating that for the data available, the assumption that the form factor is independent of the spectator quark mass is valid. Hence, the data for $\kappa_l = 0.14144$ was used for the chiral limit, to obtain $T_2(q_{max}^2; m_P; m_{K^*})$.

Bernard *et al.* [57] converted this result to $q^2=0$ by assuming single pole dominance,

$$T_2^{pole}(q^2) = \frac{T_2(0)}{1 - q^2/m_{P_{s1}}^2}. \quad (41)$$

The current J_μ in the matrix element can be expressed in a $V + A$ form, with T_1 corresponding to the vector component and T_2 and T_3 to the axial current. Therefore, in a single pole model, the exchanged particle, P_{s1} , for the T_2 form factor should be the lowest $J^P = 1^+$ state with the correct spin, parity and strangeness quantum numbers. We extracted $T_2^{pole}(q^2=0; m_P; m_{K^*})$ from $T_2(q_{max}^2)$ using a single pole model, with the mass of the 1^+ states determined from fits to two-point functions for each heavy quark mass. The results of these extrapolations are shown in the column labelled (a) in table VIII.

The ratio $T_1(q^2=0; m_P; m_{K^*})/T_2^{pole}(q^2=0; m_P; m_{K^*})$ is shown in Fig.(10). We note that using a fixed pole mass from two-point functions gives a 10-20% difference in the ratio (at the heaviest masses) compared with allowing the pole mass to vary in the fits.

B. Extrapolation to M_B

The appropriate ansatz for extrapolating the on-shell form factor in the heavy quark mass to $T_1(q^2=0; m_B; m_{K^*})$ is not *a priori* clear. As we saw in section ID, one has to model the q^2 dependence of the form factors, maintaining consistency with known heavy quark scaling results [40] at q_{max}^2 , from Eq.(15), and the relation $T_1(0) = iT_2(0)$. Expanding unknown parameters in powers of $1/m_P$, one obtains scaling laws for the on-shell form factors $T_1(q^2=0)$ and $T_2(q^2=0)$. Thus, while the scaling behaviour of $T_2(q_{max}^2)$ can be checked directly, the behaviours of $T_1(0)$ and $T_2(0)$ will depend on assumptions made for the q^2 dependence. We now address these issues.

Bernard *et al.* [57] used the heavy-quark scaling law for the off-shell form factor, $T_2(q_{max}^2; m_P; m_{K^*})$ to extrapolate T_2 to $T_2(q_{max}^2; m_B; m_{K^*})$, before applying a single pole dominance model as before to reach the on-shell point $T_2(q^2=0; m_B; m_{K^*})$. They estimated the appropriate pole mass. The validity of the pole model over the wide range of momentum transfer from $q^2=0$ to q_{max}^2 was required, but tests at heavy quark masses around the charm quark mass showed it to be quite accurate.

Our results for $T_2(q^2; m_P; m_{K^*})$, see Fig.(7), appear nearly independent of q^2 for masses m_P around the charm scale. Hence, we have fitted T_2 to both single pole and constant forms, with corresponding behaviour for T_1 . This will give us two alternative forms for the heavy mass dependence of $T_1(q^2=0; m_B; m_{K^*})$.

1. $T_2(q_{max}^2)$

At $q^2=q_{max}^2$, the initial and final hadronic states have zero spatial momentum and the contributions of form factors other than T_2 vanish,

$$\langle K^* | \bar{s} \sigma_{\mu\nu} q^\nu b_R | B \rangle = \epsilon_\mu (m_B^2 - m_{K^*}^2) T_2(q_{max}^2). \quad (42)$$

In the heavy quark limit, the matrix element of Eq.(42) scales as $m_B^{3/2}$, owing to the normalisation of the heavy quark state ($\sqrt{m_B}$) and the momentum transfer q ($q^0 = m_B - m_{K^*}$). The leading term in the heavy quark scaling of $T_2(q_{max}^2)$ is expected to be $m_B^{-1/2}$, analogous to the scaling of f_B [59,49]. Higher order $1/m_B$ and $1/m_B^2$ corrections will also be present, as will radiative corrections [60,61].

Hence, the form factor $T_2(q_{max}^2)$ should scale as,

$$T_2(q_{max}^2; m_P; m_{K^*}) \sqrt{m_P} = \text{const.} \times [\alpha_s(m_P)]^{-2/\beta_0} \left(1 + \frac{a_1}{m_P} + \frac{a_2}{m_P^2} + \dots \right). \quad (43)$$

To test heavy quark scaling, we form the quantity,

$$\hat{T}_2 = T_2(q_{max}^2) \sqrt{\frac{m_P}{m_B}} \left(\frac{\alpha_s(m_P)}{\alpha_s(m_B)} \right)^{2/\beta_0}, \quad (44)$$

where we approximate $\alpha_s(\mu)$ by,

$$\alpha_s(\mu) = \frac{2\pi}{\beta_0 \ln(\mu/\Lambda_{QCD})}. \quad (45)$$

with $\Lambda_{QCD} = 200$ MeV and $\beta_0 = 11 - \frac{2}{3}N_f$. In the quenched approximation, N_f is taken to be zero. The normalisation ensures that $\hat{T}_2 = T_2(q_{max}^2)$ at the physical mass m_B . Linear and quadratic correlated fits to Eq.(43) were carried out with the functions,

$$\hat{T}_2(m_P) = A \left(1 + \frac{B}{m_P} \right), \quad (46)$$

$$\hat{T}_2(m_P) = A \left(1 + \frac{B}{m_P} + \frac{C}{m_P^2} \right), \quad (47)$$

and are shown in Fig.(11). Taking the quadratic fit of T_2 at $m_P = m_B$ as the best estimate, and the difference between the central values of the linear and quadratic fits as an estimate of the sytematic error, T_2 was found to be

$$T_2(q_{max}^2; m_B; m_{K^*}) = 0.269_{-9}^{+17} \pm 0.011. \quad (48)$$

Once $T_2(q_{max}^2)$ is extracted, we can obtain $T_2(0)$ in the two cases, pole model or constant, for the q^2 behaviour. If T_2 is constant, then Eq.(48) is the result at $q^2 = 0$. In the pole model, the expected exchange particle for T_2 is the $1^+ B_{s1}$ state, but experimental data for its mass is not yet available. However, it is possible to estimate reasonable upper and lower bounds for the mass from HQET. It can be shown that [59],

$$m_{B_{s1}} - m_B = \Delta\bar{\Lambda} + \frac{A}{m_b} + O\left(\frac{1}{m_b^2}\right), \quad (49)$$

$$m_{D_{s1}} - m_D = \Delta\bar{\Lambda} + \frac{A}{m_c} + O\left(\frac{1}{m_c^2}\right). \quad (50)$$

Neglecting terms of order $1/m_c^2$, the upper and lower bounds for Eq.(49) are,

$$\frac{m_c}{m_b}(m_{D_{s1}} - m_D) < m_{B_{s1}} - m_B < m_{D_{s1}} - m_D \quad (51)$$

Making the approximation,

$$\frac{m_c}{m_b} \sim \frac{m_D + 3m_{D^*}}{m_B + 3m_{B^*}} \quad (52)$$

the range of the expected pole mass can be found,

$$m_{B_{s1}} = 5.74 \pm 0.21 \text{ GeV.} \quad (53)$$

Therefore,

$$T_2^{pole}(q^2=0; m_B; m_{K^*}) = 0.112_{-7}^{+7+16}_{-15}, \quad (54)$$

where the first error is statistical and the second is the systematic error obtained by combining the variation of the pole mass within its bounds and the systematic error from Eq.(48). There is clearly a significant systematic difference between the results in Eq.(48) and Eq.(54) corresponding to the two assumed forms for $T_2(q^2)$.

2. $T_1(q^2=0)$

If constant-in- q^2 behaviour is assumed for T_2 , then $T_2(0)$ should satisfy the same scaling law as $T_2(q_{max}^2)$ in Eq.(43). Combining this with the identity $T_1(0) = iT_2(0)$ leads to a scaling law for $T_1(0)$:

$$T_1(0; m_P; m_{K^*})\sqrt{m_P} = \text{const.} \times [\alpha_s(m_P)]^{-2/\beta_0} \left(1 + \frac{a_1}{m_P} + \frac{a_2}{m_P^2} + \dots \right). \quad (55)$$

If single pole dominance is assumed for T_2 and the mass of the exchanged 1^+ particle can be expanded as,

$$m_{P_{s1}} = m_P \left(1 + \frac{b_1}{m_P} + \frac{b_2}{m_P^2} + \dots \right), \quad (56)$$

then $T_1(q^2=0; m_P; m_{K^*})$ should satisfy a modified scaling law,

$$T_1(0; m_P; m_{K^*}) m_P^{3/2} = \text{const.} \times [\alpha_s(m_P)]^{-2/\beta_0} \left(1 + \frac{c_1}{m_P} + \frac{c_2}{m_P^2} + \dots \right), \quad (57)$$

where the unknown coefficients in Eq.(56) have been absorbed into the unknown scaling coefficients of the matrix element. A similar scaling relationship has been found by Ali *et al.* [19] by the sum rules approach.

The two scaling forms were tested in the same way as for $T_2(q_{max}^2)$, by forming the quantities,

$$\hat{T}_1 = T_1(q^2=0) \left(\frac{m_P}{m_B}\right)^{N/2} \left(\frac{\alpha_s(m_P)}{\alpha_s(m_B)}\right)^{2/\beta_0} . \quad (58)$$

where N is 1 or 3 as appropriate.

Linear and quadratic fits were carried out with the same functions as for \hat{T}_2 , allowing for correlations between masses and form factors. They are shown in Fig.(12). The $\chi^2/\text{d.o.f.}$ was approximately 1 for the $m_P^{3/2}$ scaling law, indicating that the model is statistically valid in the available mass range. For the $m_P^{1/2}$ scaling law we found a $\chi^2/\text{d.o.f.}$ of 0.3.

The correlated quadratic fit with radiative corrections gives,

$$T_1(q^2=0; m_B; m_{K^*}) = \begin{cases} 0.159_{-33}^{+34} & m_P^{1/2} \text{ scaling} \\ 0.124_{-18}^{+20} & m_P^{3/2} \text{ scaling} \end{cases} , \quad (59)$$

where the errors quoted are statistical.

All methods of evaluating $T_1(q^2=0; m_P; m_{K^*})$ at intermediate masses are compared in table VIII. We consider the differences between the methods as a measure of part of the systematic error. The differences between the methods of determining the form factors at the computed masses are of a similar size ($\sim 10\%$) to the systematic error at the physical B mass, as measured by the linear or quadratic extrapolation of \hat{T}_1 in the inverse heavy meson mass.

The final result for $T_1(q^2=0; m_B; m_{K^*})$ is taken from the quadratic fit for T_1 , with an estimated systematic error in extrapolation given by the difference between linear and quadratic fits,

$$T_1(q^2=0; m_B; m_{K^*}) = \begin{cases} 0.159_{-33}^{+34} \pm 0.067 & m_P^{1/2} \text{ scaling} \\ 0.124_{-18}^{+20} \pm 0.022 & m_P^{3/2} \text{ scaling} \end{cases} . \quad (60)$$

The extrapolation is shown in Fig.(12). We note that the value obtained from $m_P^{3/2}$ scaling is consistent with the corresponding value from T_2 calculated using the single pole q^2 behaviour discussed earlier.

C. $B_s \rightarrow \phi\gamma$

Much of the analysis above can also be applied to the rare decay $B_s \rightarrow \phi\gamma$. ALEPH [62] and DELPHI [63] have looked for this decay and obtained 90% CL upper bounds on its branching ratio of 4.1×10^{-4} and 1.9×10^{-3} respectively. Future research into this decay at LEP is planned. The branching ratio for this decay can be expressed in a form similar to Eq.(14),

$$BR(B_s \rightarrow \phi\gamma) = \frac{\alpha}{8\pi^4} m_b^2 G_F^2 m_{B_s}^3 \tau_{B_s} \left(1 - \frac{m_\phi^2}{m_{B_s}^2}\right)^3 |V_{tb}V_{ts}^*|^2 |C_7(m_b)|^2 |T_1^s(q^2=0)|^2, \quad (61)$$

where T_1^s is the relevant form factor from the decomposition of $\langle\phi|J_\mu|B_s\rangle$. In determining this matrix element numerically, the interpolating operator $J_\rho^V(x)$ is replaced by the operator $J_\rho^\phi(x)$ defined as,

$$J_\rho^\phi(x) = \bar{s}(x)\gamma_\rho s(x). \quad (62)$$

As a result of the presence of two identical particles in the final state, there is an extra additive term in the trace of Eq.(23), which corresponds to $\bar{s}s$ creation from purely gluonic states. It is expected that this process is heavily suppressed by Zweig's rule [64–66], and hence the extra term is neglected.

As the variation of the form factors with respect to the spectator quark mass has been discarded, it can be assumed that,

$$T_1^s(q^2=0; m_P; m_\phi) = T_1(q^2=0; m_P; m_{K^*}), \quad (63)$$

$$T_2^s(q^2=0; m_P; m_\phi) = T_2(q^2=0; m_P; m_{K^*}). \quad (64)$$

By employing the same *ansätze* for extrapolating T_1 and T_2 as the previous sections.

$$T_1^s(q^2=0; m_{B_s}; m_\phi) = \begin{cases} 0.165_{-30}^{+32} \pm 0.060 & m_P^{1/2} \text{ scaling} \\ 0.125_{-18}^{+20} \pm 0.021 & m_P^{3/2} \text{ scaling} \end{cases}, \quad (65)$$

$$T_2^s(q_{max}^2; m_{B_s}; m_\phi) = 0.270_{-9}^{+17} \pm 0.009, \quad (66)$$

$$T_2^{s,pole}(q^2=0; m_{B_s}; m_\phi) = 0.114_{-4-15}^{+7+16}. \quad (67)$$

We note that $T_1^s(q^2=0)$, with $m_P^{3/2}$ scaling, and $T_2^{s,pole}(q^2=0)$ are consistent with each other.

V. CONCLUSIONS

In this paper we have reported on an *ab initio* computation of the form factor for the decay $B \rightarrow K^*\gamma$. The large number of gauge configurations used in this calculation enables an extrapolation to the appropriate masses to be made and gives a statistically meaningful result. To compare this result with experiment we convert the preliminary branching ratio from CLEO, $BR(B \rightarrow K^*\gamma) = (4.5 \pm 1.5 \pm 0.9) \times 10^{-5}$ based on 13 events [1], into its corresponding T_1 form factor, assuming the Standard Model. We work at the scale $\mu = m_b = 4.39$ GeV, in the \overline{MS} scheme, using a pole mass of $M_b = 4.95(15)$ GeV [67] to determine m_b [68]. Taking $|V_{ts}V_{tb}| = 0.037(3)$ [69], $\tau_B = 1.5(2)$ ps [70,71] and all other values from the Particle Data Book combined with Eq.(14), we find T_1^{exp} to be 0.23(6), 0.21(5) and 0.19(5) for top quark masses of $m_t = 100, 150$ and 200 GeV respectively. We find the calculated value for T_1 consistent with these results to within two standard deviations.

In calculating the branching ratio, we use the perturbative renormalisation of $\sigma_{\mu\nu}$ [55] with a boosted coupling, $g^2 = 1.7g_0^2$, and the anomalous dimension, $\gamma_{\bar{q}\sigma q} = -(8/3)(g^2/16\pi^2)$, to match the lattice results to the continuum at the scale $\mu = m_b$, giving a matching coefficient of $Z \approx 0.95$. We apply a correction of $Z^2 = 0.90$ in the calculations below. Varying the scale of $C_7(\mu)$ from $\mu = m_b/2$ to $\mu = 2m_b$ changes the final branching ratio by +27% and -20% respectively. This is due to the perturbative calculation of $C_7(\mu)$ and future work on next-to-leading logarithmic order corrections will reduce this variation significantly [31].

These uncertainties cancel in the dimensionless hadronisation ratio, R ,

$$R = \frac{BR(B \rightarrow K^*\gamma)}{BR(B \rightarrow X_s\gamma)} \quad (68)$$

$$= 4 \left(\frac{m_B}{m_b} \right)^3 \left(1 - \frac{m_{K^*}^2}{m_B^2} \right)^3 |T_1(q^2=0)|^2, \quad (69)$$

which we find to be,

$$R = \begin{cases} \left(14.5_{-60}^{+62} (\text{stat.}) \pm 6.1 (\text{sys.}) \pm 1.6 (\text{exp.}) \right) \% & m_P^{1/2} \text{ scaling} \\ \left(8.8_{-25}^{+28} (\text{stat.}) \pm 3.0 (\text{sys.}) \pm 1.0 (\text{exp.}) \right) \% & m_P^{3/2} \text{ scaling} \end{cases}. \quad (70)$$

Assuming the recent tentative result for m_t from CDF [72], the lattice results give a branching ratio for the decay $B \rightarrow K^* \gamma$ of,

$$BR(B \rightarrow K^* \gamma) = \begin{cases} \left(2.5_{-11}^{+11} (\text{stat.}) \pm 2.1 (\text{sys.}) \pm 0.6 (\text{exp.}) \pm_{-5}^{+7} (\text{scale}) \right) \times 10^{-5} & m_P^{1/2} \text{ scaling} \\ \left(1.5_{-4}^{+5} (\text{stat.}) \pm 0.5 (\text{sys.}) \pm 0.3 (\text{exp.}) \pm_{-3}^{+4} (\text{scale}) \right) \times 10^{-5} & m_P^{3/2} \text{ scaling} \end{cases}, \quad (71)$$

where we separate the statistical and systematic errors from the lattice, experimental and theoretical (scale) uncertainties. Combining errors to produce an overall result yields,

$$BR(B \rightarrow K^* \gamma) = \begin{cases} \left(2.5 \pm 1.3 (\text{stat.}) \pm_{-26}^{+28} (\text{sys.}) \right) \times 10^{-5} & m_P^{1/2} \text{ scaling} \\ \left(1.5 \pm 0.6 (\text{stat.}) \pm_{-8}^{+9} (\text{sys.}) \right) \times 10^{-5} & m_P^{3/2} \text{ scaling} \end{cases}. \quad (72)$$

Similarly for $B_s \rightarrow \phi \gamma$, using $m_{B_s} = 5.3833(5)$ GeV [73,74] and $\tau_{B_s} = 1.54(15)$ ps [75], we find,

$$BR(B_s \rightarrow \phi \gamma) = \begin{cases} \left(2.8_{-10}^{+11} (\text{stat.}) \pm 2.1 (\text{sys.}) \pm 0.5 (\text{exp.}) \pm_{-5}^{+7} (\text{scale}) \right) \times 10^{-5} & m_P^{1/2} \text{ scaling} \\ \left(1.6_{-5}^{+5} (\text{stat.}) \pm 0.6 (\text{sys.}) \pm 0.3 (\text{exp.}) \pm_{-3}^{+4} (\text{scale}) \right) \times 10^{-5} & m_P^{3/2} \text{ scaling} \end{cases}, \quad (73)$$

$$= \begin{cases} \left(2.8 \pm 1.2 (\text{stat.}) \pm_{-26}^{+28} (\text{sys.}) \right) \times 10^{-5} & m_P^{1/2} \text{ scaling} \\ \left(1.6 \pm 0.6 (\text{stat.}) \pm_{-9}^{+10} (\text{sys.}) \right) \times 10^{-5} & m_P^{3/2} \text{ scaling} \end{cases}. \quad (74)$$

In obtaining these results, we have made some assumptions. Since this calculation is carried out with one lattice spacing, we cannot explore discretisation errors. However, the use of an $O(a)$ -improved action is expected to reduce these substantially. As the form factors and mass ratios evaluated are dimensionless, we also expect some of the systematic error from setting the scale to cancel. The extrapolation of matrix elements to the chiral limit has been neglected, although the current data indicates a weak dependence on the spectator quark mass. Without doing a simulation using dynamical fermions, the error due to quenching cannot be accurately estimated. However, the good agreement with experiment for other semileptonic, pseudoscalar to vector meson decays [41,42], that have been determined using coarser lattices and lower statistics, suggests that these errors are small. We find our results consistent with previous calculations [56,57]. With form factors available over a range of masses, we have been able to incorporate heavy-quark symmetry into our extrapolation

and investigate phenomenologically motivated pole-dominance models. These methods supercede the simple linear extrapolation used as a guide in our earlier preliminary study, where the limited set of two masses precluded an investigation of different extrapolation methods [56].

Whether pole dominance is a valid model for a large range of q^2 is an important question. We have quoted results for two different possibilities for the q^2 dependence of the form factors. Although the lattice results visually favour T_2 constant in q^2 , at least for heavy quark masses around the charm mass, our fits favour a single pole vector dominance form for T_2 . The difference between the results indicates the need for a better understanding of the combined q^2 and heavy quark scaling behaviour of the relevant form factors.

We have not applied the constraint $T_1(0) = iT_2(0)$ to our fits in this paper, using instead the consistency of our results with this relation as a guide to the fitting method. We find that the the single pole dominance model for the q^2 behaviour of T_2 (and corresponding dipole behaviour for T_1) gives the most consistent fit. In this case we have attempted to determine the systematic consistency by comparing $T_1(q^2=0; m_B; m_{K^*})$, extracted using the $m_P^{3/2}$ scaling law, with $T_2(q^2=0; m_B; m_{K^*})$ assuming pole model behaviour for T_2 and the expected pole mass. It could be argued that both methods are equivalent. However, in extrapolating the form factor $T_1(q^2=0; m_P; m_{K^*})$ to m_B , the coefficients in the fit are not fixed, which is equivalent to letting the pole mass vary. We require only that the leading order behaviour of T_1 satisfy the $m_P^{3/2}$ dependence.

We look forward to improved experimental results for the decay $B \rightarrow K^*\gamma$ and observation of $B_s \rightarrow \phi\gamma$. We hope future lattice studies will significantly increase the accuracy of these calculations.

ACKNOWLEDGMENTS

The authors wish to thank G. Martinelli for emphasising the consistency requirements on scaling the form factors T_1 and T_2 . They also thank A. Soni, C. Bernard, A. El-Khadra,

and members of the UKQCD collaboration, including C. Allton, L. Lellouch, J. Nieves and H. Wittig for useful discussions on this topic.

JMF thanks the Nuffield Foundation for support under the scheme of Awards for Newly Appointed Science Lecturers. The University of Edinburgh and the Wingate Foundation is acknowledged for its support of HPS by a scholarship. DGR (Advanced Fellow) and DSH (Personal Fellow) acknowledge the support of the Science and Engineering Research Council. The authors acknowledge the support of the Particle Physics and Astronomy Research Council by grant GR/J98202.

REFERENCES

- [1] CLEO Collaboration, R. Ammar *et al.*, Phys. Rev. Lett. **71**, 674 (1993).
- [2] S. Bertolini *et al.*, Nucl. Phys. **B353**, 591 (1991).
- [3] N. Oshimo, Nucl. Phys. **B404**, 20 (1993).
- [4] R. Barbieri and G. Giudice, Phys. Lett. B **309**, 86 (1993).
- [5] J. L. Lopez, D. V. Nanopoulos, and G. T. Park, Phys. Rev. D **48**, 974 (1993).
- [6] R. Garisto and J. N. Ng, Phys. Lett. B **315**, 372 (1993).
- [7] M. A. Diaz, Phys. Lett. B **304**, 278 (1993).
- [8] F. M. Borzumati, DESY 93-090, hep-ph 9310212 (1993).
- [9] T. G. Rizzo, Phys. Rev. D **38**, 820 (1988).
- [10] W.-S. Hou, A. Soni, and H. Steger, Phys. Lett. B **192**, 441 (1987).
- [11] J. L. Hewett, SLAC-PUB-6521, hep-ph 9406302 (1994).
- [12] N. G. Deshpande, P. Lo, and J. Trampetic, Z. Phys. **C40**, 369 (1988).
- [13] P. J. O'Donnell and H. K. K. Tung, Phys. Rev. D **44**, 741 (1991).
- [14] T. Altomari, Phys. Rev. D **37**, 677 (1988).
- [15] C. A. Dominguez, N. Paver, and Riazuddin, Phys. Lett. B **214**, 459 (1988).
- [16] T. M. Aliev, A. A. Ovchinnikov, and V. A. Slobodenyuk, Phys. Lett. B **237**, 569 (1990).
- [17] P. Ball, TUM-T31-43-93, hep-ph 9308244 (1993).
- [18] P. Colangelo, C. A. Dominguez, G. Nardulli, and N. Paver, Phys. Lett. B **317**, 183 (1993).
- [19] A. Ali, V. M. Braun, and H. Simma., CERN-TH-7118-93, MPI-Ph/93-97, DESY 93-

- 193, hep-ph 9401277 (1993).
- [20] S. Narison, Phys. Lett. B **324**, 354 (1994).
- [21] A. Ali, T. Mannel, and T. Ohl, Phys. Lett. B **298**, 195 (1993).
- [22] C. W. Bernard, P. F. Hsieh, and A. Soni, Nucl. Phys. (Proc Suppl.) **B26**, 347 (1992),
note that there is a factor of 2 missing in eq. (4) of this paper.
- [23] P. Cho and M. Misiak, CALT-68-1893, TUM-T31-52/93, hep-ph 9310332 (1993).
- [24] L. Randall and R. Sundrum, Phys. Lett. B **312**, 148 (1993).
- [25] S. Chia, Phys. Lett. B **240**, 465 (1990).
- [26] K. Peterson, Phys. Lett. B **282**, 207 (1992).
- [27] T. Rizzo, Phys. Lett. B **315**, 471 (1993).
- [28] X.-G. He and B. McKellar, Phys. Lett. B **320**, 165 (1994).
- [29] S. Glashow and S. Weinberg, Phys. Rev. D **21**, 1393 (1980).
- [30] L. F. Abbot, P. Sikivie, and M. B. Wise, Phys. Rev. D **21**, 1393 (1980).
- [31] A. Buras, M. Misiak, M. Münz, and S. Pokorski, MPI-Ph/93-77, TUM-T31-50/93,
hep-ph 9311345 (1993).
- [32] J. L. Hewett, Phys. Rev. Lett. **70**, 1045 (1993).
- [33] M. A. Diaz, Phys. Lett. **B322**, 207 (1994), hep-ph 9311228.
- [34] A. F. Falk, M. Luke, and M. J. Savage, (1993), hep-ph 9308288.
- [35] CLEO Collaboration, B. Barish *et al.*, CLEO CONF 94-1 (1994).
- [36] B. Grinstein, R. Springer, and M. B. Wise, Nucl. Phys. **B339**, 269 (1990).
- [37] H. Simma, DESY-93-083, hep-ph 9307274 (1993).

- [38] M. Ciuchini *et al.*, Phys. Lett. B **316**, 127 (1993).
- [39] P. Cho and B. Grinstein, Nucl. Phys. **B365**, 279 (1991).
- [40] N. Isgur and M. B. Wise, Phys. Rev. D **42**, 2388 (1990).
- [41] V. Lubicz *et al.*, Phys. Lett. B **274**, 415 (1992).
- [42] C. Bernard, A. El-Khadra, and A. Soni, Phys. Rev. D **45**, 869 (1992).
- [43] UKQCD collaboration, D. Richards *et al.*, Nucl. Phys. (Proc. Suppl.) **34**, 411 (1994).
- [44] M. Lüscher and P. Weisz, Commun. Math. Phys. **97**, 59 (1985).
- [45] UKQCD Collaboration, C. Allton *et al.*, Nucl. Phys. **B407**, 331 (1993).
- [46] B. Sheikholeslami and R. Wohlert, Nucl. Phys. **B259**, 572 (1985).
- [47] K. G. Wilson, in *New Phenomena in Subnuclear Physics*, edited by A. Zichichi (Plenum, New York, 1977).
- [48] G. Heatlie *et al.*, Nucl. Phys. **B352**, 266 (1991).
- [49] UKQCD Collaboration, R. M. Baxter *et al.*, Phys. Rev. D **49**, 1594 (1994).
- [50] C. Allton *et al.*, Phys. Lett. **B292**, 408 (1992), hep-lat 9208018.
- [51] UKQCD Collaboration, C. Allton *et al.*, Phys. Rev. D **49**, 474 (1994).
- [52] UKQCD Collaboration, C. Allton *et al.*, Phys. Rev. D **47**, 5128 (1993).
- [53] D. Daniel *et al.*, Phys. Rev. D **46**, 3130 (1992).
- [54] B. Efron, SIAM Review **21**, 460 (1979).
- [55] A. Borrelli, C. Pittori, R. Frezzotti, and E. Gabrielli, Nucl. Phys. **B409**, 382 (1993).
- [56] UKQCD Collaboration, K. C. Bowler *et al.*, Phys. Rev. Lett. **72**, 1398 (1994), hep-lat 9311004.

- [57] C. Bernard, P. Hsieh, and A. Soni, Phys. Rev. Lett. **72**, 1402 (1994), hep-lat 9311011.
- [58] UKQCD Collaboration, C. Allton *et al.*, Edinburgh preprint 93/524, Southampton preprint SHEP 92/93-16, hep-lat 9309002 (1993).
- [59] M. Neubert, SLAC-PUB-6263, hep-ph 9306320 (1993).
- [60] M. Voloshin and M. Shifman, Sov. J. Nucl. Phys. **45**, 292 (1987).
- [61] H. Politzer and M. B. Wise, Phys. Lett. **206B**, 681 (1988).
- [62] ALEPH collaboration, A. Bonnssent *et al.*, talk given at the 28th Rencontres de Moriond (1993).
- [63] DELPHI collaboration, M. Battaglia *et al.*, Helsinki University Report No. HU SEFT R 1993-14 , to appear in the proceedings of the 5th International Symposium on Heavy Flavour Physics 1993.
- [64] G. Zweig, CERN report no. 8419/TH 412 (1964).
- [65] S. Okubo, Phys. Lett. **5**, 163 (1963).
- [66] J. Iizuka, Prog. Theor. Phys. Suppl. **37**, 21 (1966).
- [67] NRQCD collaboration, C.T.H. Davies *et al.*, hep-lat 9404012 (1994).
- [68] N. Gray, D. Broadhurst, W. Grafe, and K. Schilcher, Z. Phys. **C48**, 673 (1990).
- [69] S. Stone, in *B Decays*, edited by S. Stone (World Scientific, Singapore, 1994), (2nd Ed., to be published).
- [70] ALEPH Collaboration, D. Buskulic *et al.*, Phys. Lett. **B307**, 194 (1993).
- [71] OPAL collaboration, P.D. Acton *et al.*, Phys. Lett. **B307**, 247 (1993).
- [72] CDF Collaboration, F. Abe *et al.*, Fermilab Pub 94/097-E .
- [73] OPAL Collaboration, D. Buskulic *et al.*, Phys. Lett. **B311**, 425 (1993), erratum-ibid.

B316:631,1993.

[74] CDF Collaboration, F. Abe *et al.*, Phys. Rev. Lett. **71**, 1685 (1993).

[75] R. Forty, to appear in Proc. of XIV Int. Conf. on Physics in Collision, Tallahassee, June 15-17 (1994).

TABLES

κ_h	κ_s	κ_l	low $(qa)^2$	high $(qa)^2$	$T_1(0)$	$\chi^2/\text{d.o.f.}$
0.12100	0.14144	0.14144	-0.032_{-6}^{+7}	0.258_{-9}^{+7}	0.283_{-12}^{+19}	11.2/3
0.12100	0.14144	0.14226	-0.035_{-9}^{+9}	0.265_{-12}^{+11}	0.282_{-21}^{+30}	8.8/3
0.12100	0.14144	0.14262	-0.035_{-12}^{+12}	0.271_{-16}^{+15}	0.294_{-36}^{+44}	4.1/3
0.12100	0.14226	0.14144	-0.014_{-9}^{+10}	0.290_{-13}^{+10}	0.271_{-17}^{+24}	7.3/3
0.12100	0.14226	0.14226	-0.022_{-15}^{+16}	0.298_{-18}^{+17}	0.279_{-40}^{+40}	6.7/3
0.12100	0.14226	0.14262	-0.028_{-22}^{+22}	0.306_{-26}^{+24}	0.294_{-71}^{+58}	4.2/3
0.12500	0.14144	0.14144	-0.118_{-5}^{+5}	0.157_{-7}^{+6}	0.307_{-9}^{+17}	10.3/3
0.12500	0.14226	0.14144	-0.104_{-7}^{+8}	0.183_{-10}^{+9}	0.292_{-13}^{+21}	8.5/3
0.12900	0.14144	0.14144	-0.188_{-4}^{+4}	0.086_{-4}^{+4}	0.335_{-8}^{+18}	9.4/3
0.12900	0.14144	0.14226	-0.190_{-5}^{+6}	0.084_{-5}^{+6}	0.333_{-12}^{+23}	7.2/3
0.12900	0.14144	0.14262	-0.190_{-6}^{+8}	0.084_{-6}^{+8}	0.336_{-21}^{+30}	3.2/3
0.12900	0.14226	0.14144	-0.177_{-5}^{+6}	0.097_{-5}^{+6}	0.318_{-10}^{+18}	7.1/3
0.12900	0.14226	0.14226	-0.182_{-8}^{+10}	0.096_{-12}^{+12}	0.319_{-19}^{+27}	7.5/3
0.12900	0.14226	0.14262	-0.186_{-12}^{+14}	0.103_{-17}^{+17}	0.324_{-30}^{+37}	3.6/3
0.13300	0.14144	0.14144	-0.240_{-2}^{+3}	0.034_{-2}^{+3}	0.366_{-9}^{+19}	7.3/3
0.13300	0.14226	0.14144	-0.233_{-3}^{+4}	0.041_{-3}^{+4}	0.343_{-10}^{+21}	5.7/3

TABLE I. Results of pole fits to $T_1(q^2; m_P; m_V)$.

κ_h	κ_s	κ_l	low $(qa)^2$	high $(qa)^2$	$T_1(0)$	$\chi^2/\text{d.o.f.}$
0.12100	0.14144	0.14144	-0.032^{+7}_{-6}	0.258^{+7}_{-9}	0.279^{+20}_{-12}	9.2/3
0.12100	0.14144	0.14226	-0.035^{+9}_{-9}	0.265^{+11}_{-12}	0.275^{+32}_{-24}	7.8/3
0.12100	0.14144	0.14262	-0.035^{+12}_{-12}	0.271^{+15}_{-16}	0.286^{+46}_{-36}	3.5/3
0.12100	0.14226	0.14144	-0.014^{+10}_{-9}	0.290^{+10}_{-13}	0.266^{+26}_{-19}	6.4/3
0.12100	0.14226	0.14226	-0.022^{+16}_{-15}	0.298^{+17}_{-18}	0.274^{+43}_{-42}	6.5/3
0.12100	0.14226	0.14262	-0.028^{+22}_{-22}	0.306^{+24}_{-26}	0.286^{+67}_{-66}	3.9/3
0.12500	0.14144	0.14144	-0.118^{+5}_{-5}	0.157^{+6}_{-7}	0.308^{+18}_{-9}	8.6/3
0.12500	0.14226	0.14144	-0.104^{+8}_{-7}	0.183^{+9}_{-10}	0.291^{+21}_{-14}	7.3/3
0.12900	0.14144	0.14144	-0.188^{+4}_{-4}	0.086^{+4}_{-4}	0.337^{+18}_{-8}	7.9/3
0.12900	0.14144	0.14226	-0.190^{+6}_{-5}	0.084^{+6}_{-5}	0.334^{+23}_{-12}	6.5/3
0.12900	0.14144	0.14262	-0.190^{+8}_{-6}	0.084^{+8}_{-6}	0.337^{+30}_{-20}	2.7/3
0.12900	0.14226	0.14144	-0.177^{+6}_{-5}	0.097^{+6}_{-5}	0.319^{+18}_{-10}	5.8/3
0.12900	0.14226	0.14226	-0.182^{+10}_{-8}	0.096^{+12}_{-12}	0.320^{+27}_{-19}	6.8/3
0.12900	0.14226	0.14262	-0.186^{+14}_{-12}	0.103^{+17}_{-17}	0.325^{+37}_{-30}	3.2/3
0.13300	0.14144	0.14144	-0.240^{+3}_{-2}	0.034^{+3}_{-2}	0.362^{+19}_{-9}	6.2/3
0.13300	0.14226	0.14144	-0.233^{+4}_{-3}	0.041^{+4}_{-3}	0.341^{+20}_{-10}	4.4/3

TABLE II. Results of dipole fits to $T_1(q^2; m_P; m_V)$.

κ_h	κ_s	κ_l	low $(qa)^2$	high $(qa)^2$	$T_2(0)$	$\chi^2/\text{d.o.f.}$
0.12100	0.14144	0.14144	-0.032_{-6}^{+7}	0.289_{-7}^{+6}	0.301_{-12}^{+22}	6.4/4
0.12100	0.14144	0.14226	-0.035_{-9}^{+9}	0.293_{-10}^{+9}	0.310_{-23}^{+32}	7.5/4
0.12100	0.14144	0.14262	-0.035_{-12}^{+12}	0.297_{-15}^{+13}	0.315_{-39}^{+44}	8.8/4
0.12100	0.14226	0.14144	-0.014_{-9}^{+10}	0.318_{-11}^{+9}	0.288_{-17}^{+25}	4.4/4
0.12100	0.14226	0.14226	-0.022_{-15}^{+16}	0.324_{-16}^{+15}	0.300_{-31}^{+38}	5.6/4
0.12100	0.14226	0.14262	-0.028_{-22}^{+22}	0.330_{-25}^{+22}	0.312_{-67}^{+52}	5.6/4
0.12500	0.14144	0.14144	-0.118_{-5}^{+5}	0.190_{-6}^{+5}	0.322_{-10}^{+19}	4.3/4
0.12500	0.14226	0.14144	-0.104_{-7}^{+8}	0.214_{-9}^{+8}	0.310_{-13}^{+22}	3.7/4
0.12900	0.14144	0.14144	-0.188_{-4}^{+4}	0.108_{-4}^{+3}	0.351_{-8}^{+17}	7.9/4
0.12900	0.14144	0.14226	-0.190_{-5}^{+6}	0.109_{-6}^{+6}	0.353_{-12}^{+23}	6.9/4
0.12900	0.14144	0.14262	-0.190_{-6}^{+8}	0.112_{-9}^{+8}	0.349_{-20}^{+30}	10.7/4
0.12900	0.14226	0.14144	-0.177_{-5}^{+6}	0.126_{-7}^{+6}	0.332_{-10}^{+19}	5.2/4
0.12900	0.14226	0.14226	-0.182_{-8}^{+10}	0.129_{-10}^{+9}	0.337_{-20}^{+28}	6.8/4
0.12900	0.14226	0.14262	-0.186_{-12}^{+14}	0.133_{-15}^{+14}	0.336_{-34}^{+36}	12.4/4
0.13300	0.14144	0.14144	-0.240_{-2}^{+3}	0.045_{-3}^{+2}	0.372_{-6}^{+14}	7.7/4
0.13300	0.14226	0.14144	-0.233_{-3}^{+4}	0.057_{-5}^{+4}	0.351_{-7}^{+16}	7.5/4

TABLE III. Results of pole fits to $T_2(q^2; m_P; m_V)$.

κ_h	κ_s	κ_l	low $(qa)^2$	high $(qa)^2$	$T_2(0)$	$\chi^2/\text{d.o.f.}$
0.12100	0.14144	0.14144	-0.032_{-6}^{+7}	0.289_{-7}^{+6}	0.344_{-5}^{+15}	18.4/5
0.12100	0.14144	0.14226	-0.035_{-9}^{+9}	0.293_{-10}^{+9}	0.334_{-8}^{+19}	8.6/5
0.12100	0.14144	0.14262	-0.035_{-12}^{+12}	0.297_{-15}^{+13}	0.322_{-13}^{+23}	8.8/5
0.12100	0.14226	0.14144	-0.014_{-9}^{+10}	0.318_{-11}^{+9}	0.323_{-6}^{+16}	8.6/5
0.12100	0.14226	0.14226	-0.022_{-15}^{+16}	0.324_{-16}^{+15}	0.323_{-10}^{+22}	6.2/5
0.12100	0.14226	0.14262	-0.028_{-22}^{+22}	0.330_{-25}^{+22}	0.314_{-17}^{+28}	5.6/5
0.12500	0.14144	0.14144	-0.118_{-5}^{+5}	0.190_{-6}^{+5}	0.353_{-6}^{+15}	16.4/5
0.12500	0.14226	0.14144	-0.104_{-7}^{+8}	0.214_{-9}^{+8}	0.333_{-6}^{+16}	6.6/5
0.12900	0.14144	0.14144	-0.188_{-4}^{+4}	0.108_{-4}^{+3}	0.365_{-5}^{+15}	12.6/5
0.12900	0.14144	0.14226	-0.190_{-5}^{+6}	0.109_{-6}^{+6}	0.361_{-8}^{+20}	7.5/5
0.12900	0.14144	0.14262	-0.190_{-6}^{+8}	0.112_{-9}^{+8}	0.353_{-12}^{+24}	10.8/5
0.12900	0.14226	0.14144	-0.177_{-5}^{+6}	0.126_{-7}^{+6}	0.342_{-5}^{+15}	6.2/5
0.12900	0.14226	0.14226	-0.182_{-8}^{+10}	0.129_{-10}^{+9}	0.339_{-9}^{+21}	6.9/5
0.12900	0.14226	0.14262	-0.186_{-12}^{+14}	0.133_{-15}^{+14}	0.335_{-16}^{+30}	12.4/5
0.13300	0.14144	0.14144	-0.240_{-2}^{+3}	0.045_{-3}^{+2}	0.374_{-6}^{+14}	8.5/5
0.13300	0.14226	0.14144	-0.233_{-3}^{+4}	0.057_{-5}^{+4}	0.351_{-5}^{+15}	7.5/5

TABLE IV. Results of constant fits to $T_2(q^2; m_P; m_V)$.

		$T_1(m_q) = a + bm_q$			$T_1(m_q) = c$	
κ_h	κ_s	a	b	$\chi^2/\text{d.o.f.}$	c	$\chi^2/\text{d.o.f.}$
0.121	0.14144	0.299^{+40}_{-33}	-0.362^{+677}_{-626}	0.04/1	0.281^{+18}_{-12}	0.3/2
0.121	0.14226	0.289^{+59}_{-54}	-0.326^{+100}_{-104}	0.05/1	0.271^{+21}_{-12}	0.1/2
0.121	0.1419	0.293^{+49}_{-42}			0.275^{+19}_{-12}	
0.129	0.14144	0.336^{+27}_{-16}	-0.058^{+352}_{-391}	0.1/1	0.333^{+18}_{-9}	0.1/2
0.129	0.14226	0.330^{+30}_{-21}	-0.288^{+403}_{-413}	0.2/1	0.316^{+17}_{-9}	0.8/2
0.129	0.1419	0.333^{+27}_{-18}			0.324^{+17}_{-9}	

TABLE V. Extrapolation of $T_1(q^2 = 0)$, from a single pole fit, to the chiral limit, where T_1 is assumed either to have a linear dependence on the pole mass of the light quark, or to be independent of the pole mass. $\kappa_{strange} = 0.1419$ corresponds to the physical strange quark mass from determining the mass of the K on this lattice.

		$T_2(q^2=0; m_q) = a + bm_q$			$T_2(q^2=0; m_q) = c$	
κ_h	κ_s	a	b	$\chi^2/\text{d.o.f.}$	c	$\chi^2/\text{d.o.f.}$
0.12900	0.14144	0.363^{+22}_{-24}	-0.311^{+460}_{-394}	0.1/1	0.348^{+13}_{-9}	0.6/2
0.12900	0.14226	0.337^{+23}_{-31}	-0.190^{+713}_{-396}	0.1/1	0.329^{+17}_{-9}	0.3/2
0.12900	0.14190	0.349^{+22}_{-27}			0.337^{+15}_{-9}	
0.12100	0.14144	0.323^{+32}_{-43}	-0.406^{+826}_{-596}	0.01/1	0.304^{+17}_{-14}	0.3/2
0.12100	0.14226	0.311^{+23}_{-47}	-0.531^{+1008}_{-452}	0.1/1	0.289^{+19}_{-15}	0.6/2
0.12100	0.14190	0.317^{+25}_{-42}			0.296^{+18}_{-15}	

TABLE VI. Extrapolation of $T_2(q^2=0)$, from a single pole fit, to the chiral limit, where T_2 is assumed either to have a linear dependence on the pole mass of the light quark, or to be independent of the pole mass. $\kappa_{strange} = 0.1419$ corresponds to the physical strange quark mass from determining the mass of the K on this lattice.

		$T_2(q_{max}^2; m_q) = a + bm_q$			$T_2(q_{max}^2; m_q) = c$	
κ_h	κ_s	a	b	$\chi^2/\text{d.o.f.}$	c	$\chi^2/\text{d.o.f.}$
0.12100	0.14144	0.331_{-14}^{+29}	0.492_{-434}^{+348}	0.4/1	0.353_{-7}^{+15}	1.9/2
0.12100	0.14226	0.327_{-17}^{+31}	-0.026_{-466}^{+378}	1.9/1	0.325_{-6}^{+15}	1.9/2
0.12100	0.14190	0.328_{-16}^{+29}			0.337_{-6}^{+15}	
0.12900	0.14144	0.370_{-10}^{+27}	-0.136_{-368}^{+198}	0.9/1	0.363_{-6}^{+13}	1.1/2
0.12900	0.14226	0.349_{-16}^{+32}	-0.136_{-453}^{+308}	0.7/1	0.341_{-6}^{+13}	0.8/2
0.12900	0.14190	0.358_{-13}^{+29}			0.351_{-6}^{+13}	

TABLE VII. Extrapolation of $T_2(q_{max}^2)$ to the chiral limit, where T_2 is assumed either to have a linear dependence on the pole mass of the light quark, or to be independent of the pole mass. $\kappa_{strange} = 0.1419$ corresponds to the physical strange quark mass from determining the mass of the K on this lattice.

κ_h	m_{K^*}/m_P	$T_2(q_{max}^2)$	$q_{max}^2/m_{P_{s1}}^2$	$T_2(0)$ (a)	$T_1(0)$ (b)	$T_1(0)$ (c)	$T_2(0)$ (d)	$T_2(0)$ (e)
0.13300	0.59_{-2}^{+2}	0.362_{-6}^{+15}	0.08_{-1}^{+1}	0.333_{-7}^{+14}	0.356_{-10}^{+19}	0.353_{-8}^{+19}	0.359_{-7}^{+15}	0.361_{-4}^{+14}
0.12900	0.48_{-2}^{+2}	0.353_{-6}^{+15}	0.15_{-1}^{+1}	0.301_{-7}^{+14}	0.324_{-9}^{+19}	0.326_{-7}^{+17}	0.339_{-9}^{+17}	0.352_{-4}^{+15}
0.12500	0.42_{-2}^{+2}	0.346_{-6}^{+16}	0.20_{-1}^{+1}	0.276_{-7}^{+14}	0.298_{-11}^{+19}	0.298_{-10}^{+19}	0.318_{-12}^{+20}	0.342_{-5}^{+15}
0.12100	0.37_{-1}^{+2}	0.339_{-7}^{+16}	0.26_{-1}^{+2}	0.252_{-8}^{+14}	0.278_{-14}^{+22}	0.276_{-13}^{+22}	0.298_{-15}^{+23}	0.332_{-4}^{+15}
	0.1692_{-1}^{+1}	0.269_{-9}^{+17}	0.51_{-6}^{+6}	0.112_{-7}^{+7}	0.124_{-18}^{+20}	0.159_{-33}^{+34}		

TABLE VIII. Comparison of results from different methods of extracting $T_{1,2}(q^2=0)$. The last row indicates the final extrapolation to the physical regime m_{K^*}/m_B , with results of the three methods of extracting $T_{1,2}(q^2=0; m_B; m_{K^*})$ at the feet of columns labelled (a), (b) and (c). Column labels: (a) pole form, with 1^+ mass from two-point functions [estimated from B_{s1} mass for final extrapolation], (b) dipole form, with $m_P^{3/2}$ scaling for final extrapolation, (c) pole form, with $m_P^{1/2}$ scaling for final extrapolation, (d) pole form, with mass determined from pole fit, (e) constant form factor.

FIGURES

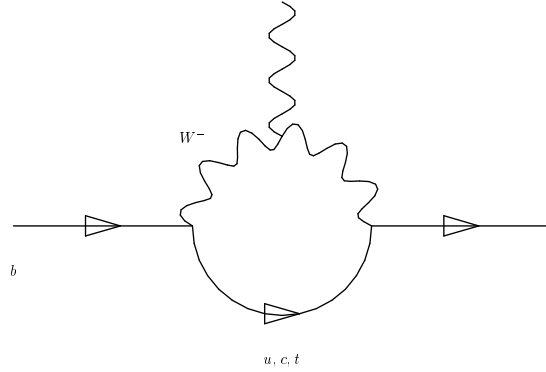


FIG. 1. An example of a penguin diagram contributing to the decay $b \rightarrow s\gamma$.

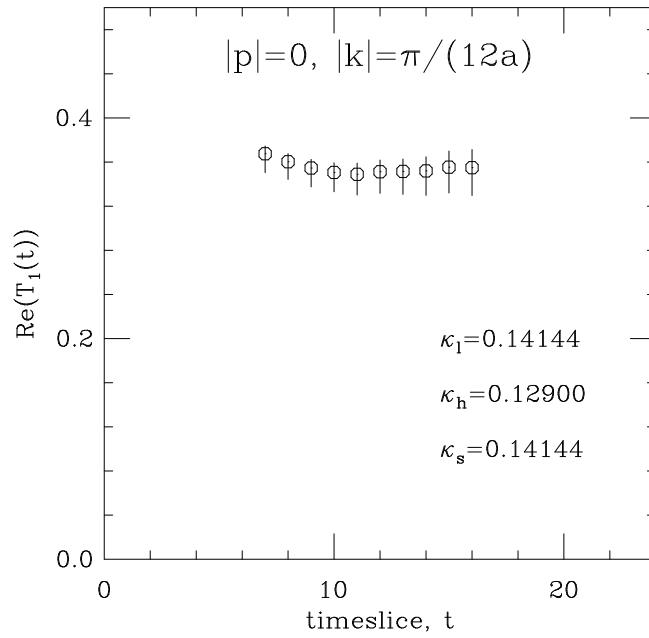


FIG. 2. A typical plot of $T_1(q^2=0; m_P; m_V)$ vs. time. From the application of the time reversal operator, it can be shown that only the real component of T_1 is non-zero.

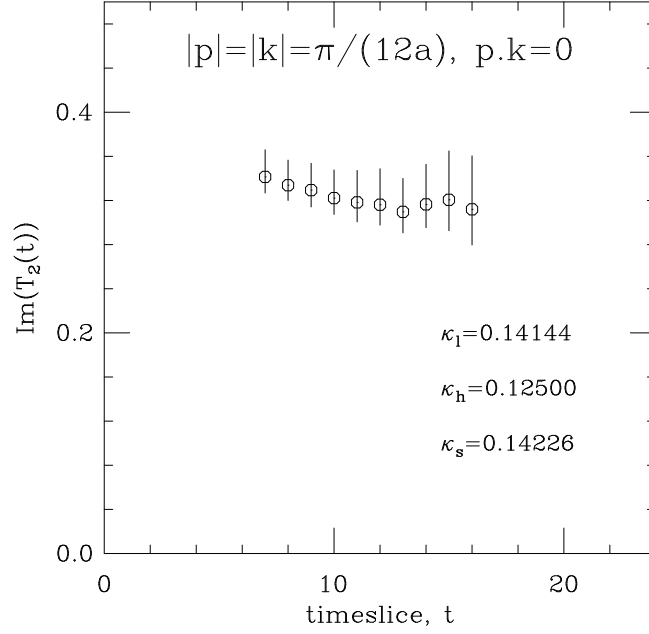


FIG. 3. $\text{Im}(T_2)$, for a typical momentum used. From the application of the time reversal operator, it can be shown that only the imaginary component of T_2 is non-zero.

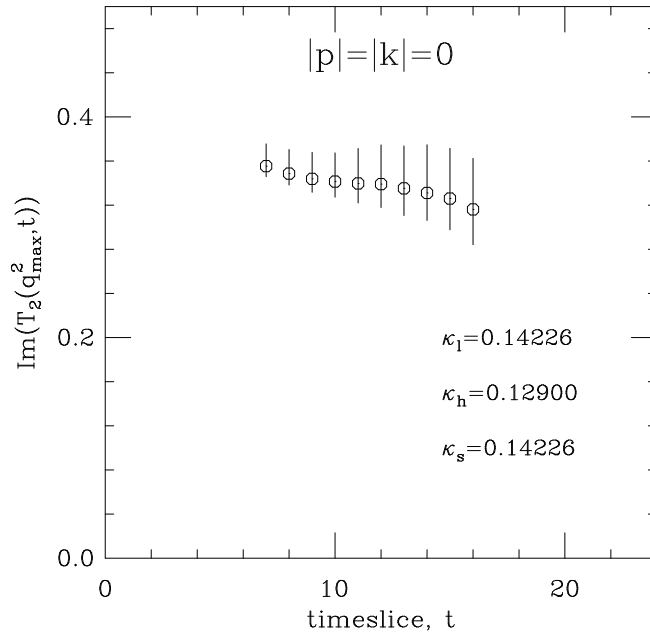


FIG. 4. A typical plot of $T_2(q_{max}^2; m_P; m_V)$ vs. time.

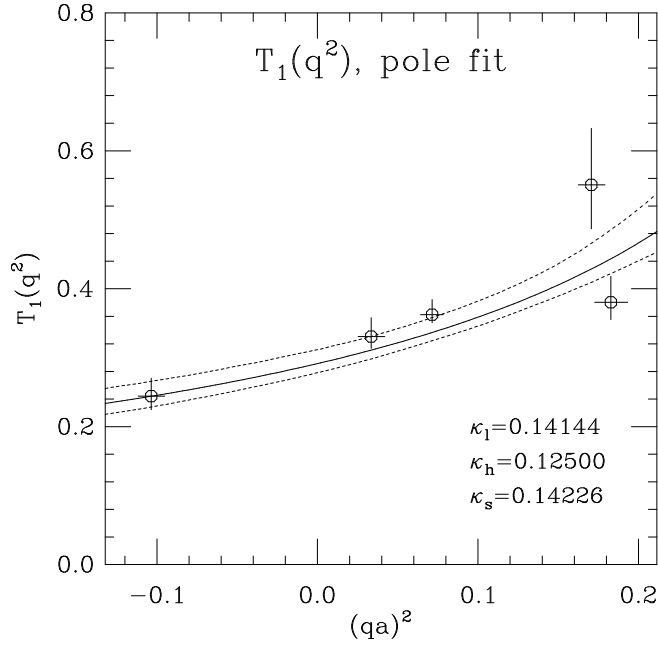


FIG. 5. $T_1(q^2)$, using a pole fit. The dotted lines represent the 68% confidence levels of the fit at each q^2 .

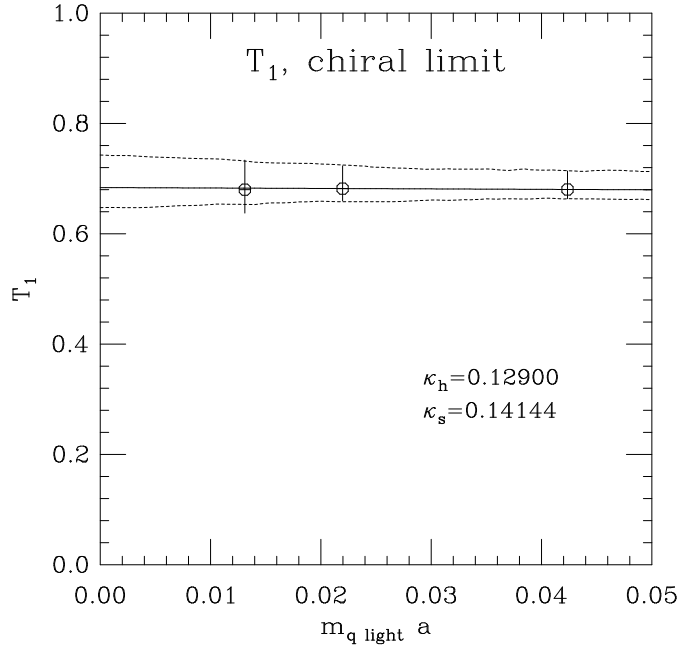


FIG. 6. Chiral extrapolation of $T_1(q^2=0)$. The dotted lines indicate the 68% confidence levels of the fit. $am_q \text{ light}$ is the lattice pole mass.

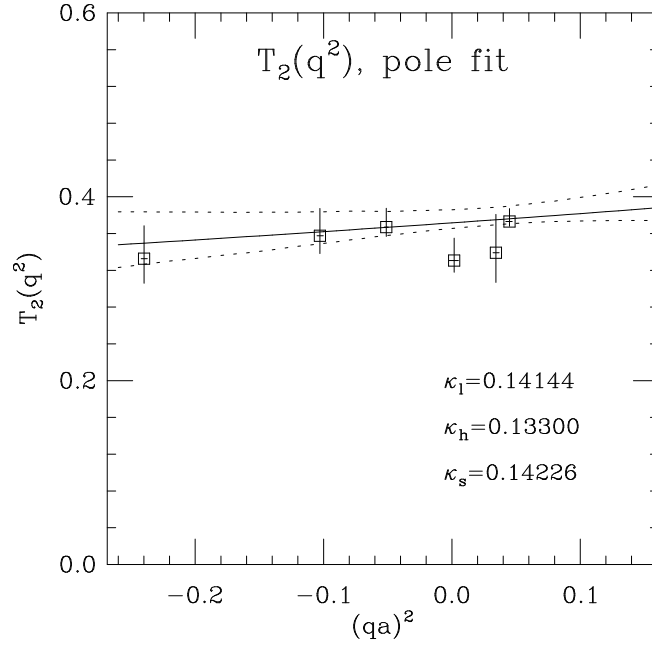


FIG. 7. $T_2(q^2)$, with a pole fit. The dotted lines represent the 68% confidence levels of the fit at each q^2 .

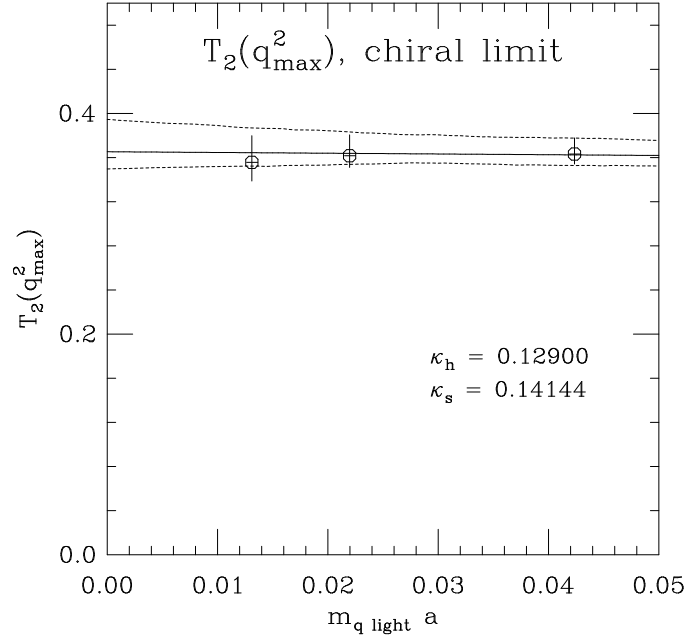


FIG. 8. Chiral extrapolation of $T_2(q_{\max}^2)$.

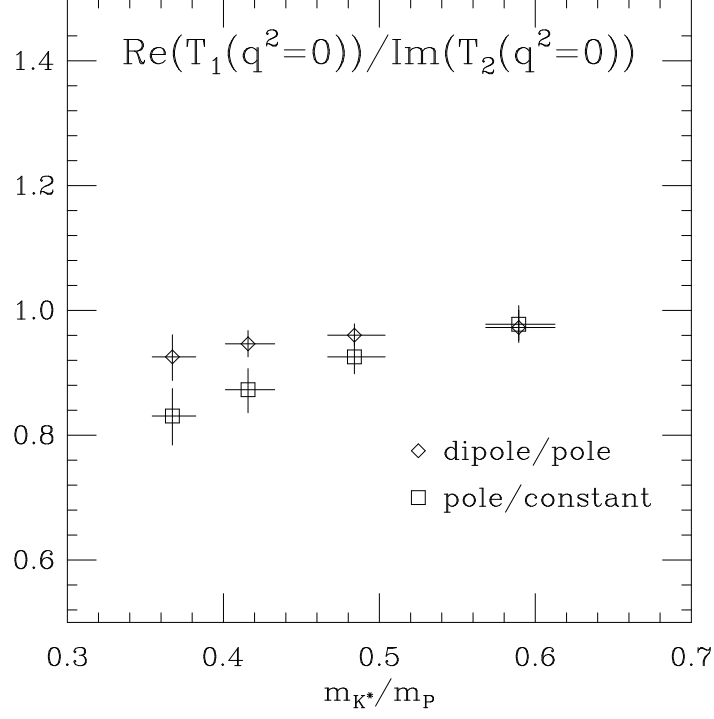


FIG. 9. The ratio T_1/T_2 at $q^2=0$ for dipole/pole and pole/constant fits.

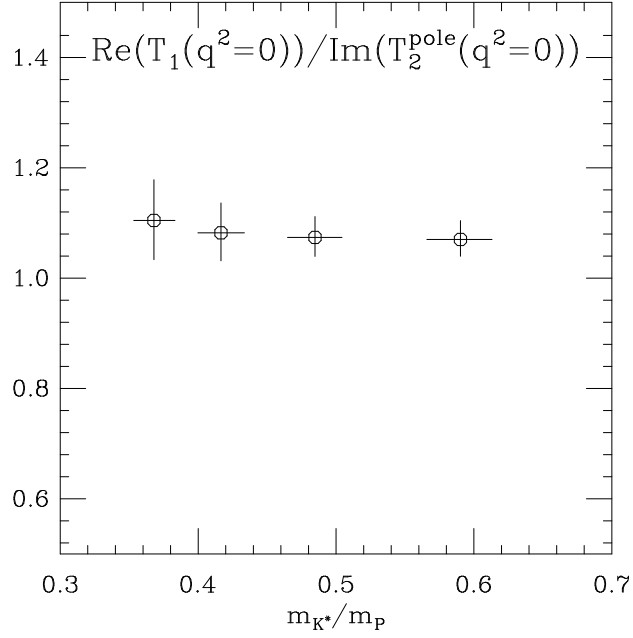


FIG. 10. The ratio $T_1(q^2=0; m_P; m_{K^*})/T_2^{pole}(q^2=0; m_P; m_{K^*})$ with T_1 fitted to a dipole form and T_2^{pole} extrapolated from $T_2(q_{max}^2)$ using a fitted 1^+ mass.

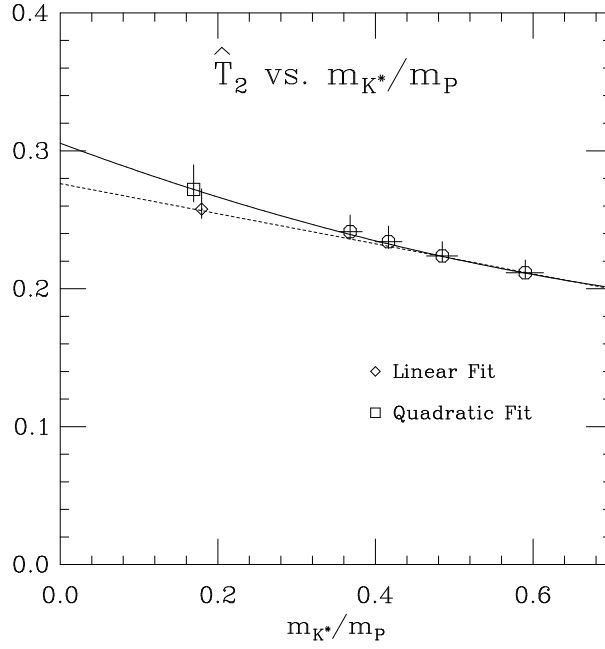


FIG. 11. Extrapolation of $T_2(q_{max}^2)$ to m_B , assuming HQET. The quantity plotted is \hat{T}_2 , defined in the text, which is equal to $T_2(q_{max}^2)$ at m_B .

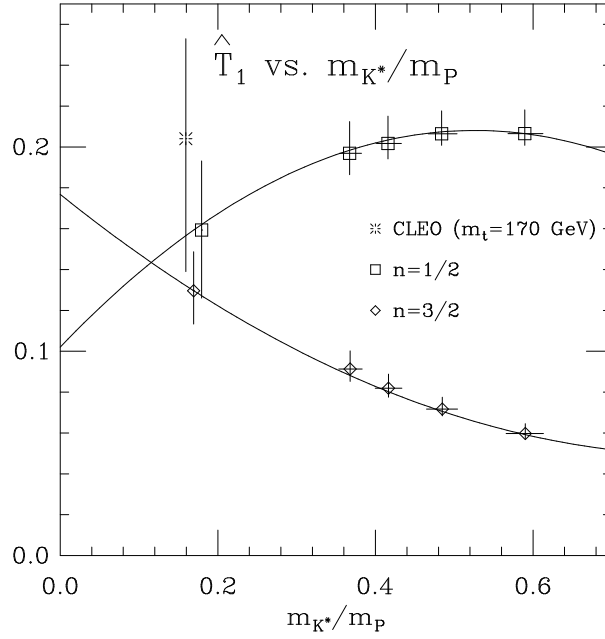


FIG. 12. \hat{T}_1 extrapolation, for $N = 1/2, 3/2$ (Points at m_{K^*}/m_B displaced slightly for clarity). \hat{T}_1 is defined in the text and agrees with $T_1(q^2=0)$ at m_B for both $N = 1/2, 3/2$. The CLEO point is obtained from the CLEO measurement of $BR(B \rightarrow K^*\gamma)$ as explained in the text.

This figure "fig1-1.png" is available in "png" format from:

<http://arxiv.org/ps/hep-lat/9407013v2>

This figure "fig2-1.png" is available in "png" format from:

<http://arxiv.org/ps/hep-lat/9407013v2>

This figure "fig3-1.png" is available in "png" format from:

<http://arxiv.org/ps/hep-lat/9407013v2>

This figure "fig1-2.png" is available in "png" format from:

<http://arxiv.org/ps/hep-lat/9407013v2>

This figure "fig2-2.png" is available in "png" format from:

<http://arxiv.org/ps/hep-lat/9407013v2>

This figure "fig3-2.png" is available in "png" format from:

<http://arxiv.org/ps/hep-lat/9407013v2>

This figure "fig1-3.png" is available in "png" format from:

<http://arxiv.org/ps/hep-lat/9407013v2>

This figure "fig2-3.png" is available in "png" format from:

<http://arxiv.org/ps/hep-lat/9407013v2>

This figure "fig3-3.png" is available in "png" format from:

<http://arxiv.org/ps/hep-lat/9407013v2>

This figure "fig1-4.png" is available in "png" format from:

<http://arxiv.org/ps/hep-lat/9407013v2>

This figure "fig2-4.png" is available in "png" format from:

<http://arxiv.org/ps/hep-lat/9407013v2>

This figure "fig3-4.png" is available in "png" format from:

<http://arxiv.org/ps/hep-lat/9407013v2>

This figure "fig1-5.png" is available in "png" format from:

<http://arxiv.org/ps/hep-lat/9407013v2>

This figure "fig2-5.png" is available in "png" format from:

<http://arxiv.org/ps/hep-lat/9407013v2>